2018 IEEE 68th Electronic Components and Technology Conference

Low-Temperature Assembly of Surface-Mount Device on Flexible Substrate using Additive Printing Process

Christine L. Taylor[1], Xuanke He[2], Vanessa Smet[3],
Manos M. Tentzeris[2], and Suresh K. Sitaraman[1]

[1] George W. Woodruff School of Mechanical Eng.
Georgia Institute of Technology
Atlanta, GA, USA
Suresh.Sitaraman@me.gatech.edu

[2]School of Electrical and Computer Eng.
Georgia Institute of Technology, Atlanta, GA USA

[3] 3D Systems Packaging Research Center
Georgia Institute of Technology, Atlanta, GA USA

Abstract— **Flexible substrates with printed electronics and surface-mount devices are being increasingly explored for various applications. For the assembly of surface-mount devices, conductive adhesives and films are being thought of as suitable alternatives to solder reflow assembly. However, such assemblies face many performance limitations particularly at high frequencies, and process limitations when the surface-mount devices are thin. This paper presents an innovative, low-temperature ink-to-ink fully-additive sintering process for surface-mount device assembly on a liquid crystal polymer (LCP) substrate with printed Ag pads. The printed ink is characterized using tape peel and button shear tests. Upon assembly of a surface-mount device, the strength of the device-to-substrate joint is assessed through a die shear test, and it is seen that the joint is stronger than the adhesion of the printed conductor to the flexible substrate. Thus, the proposed fully-additive assembly process appears to be a viable assembly method for attaching surface-mount devices on flexible substrates.**

Keywords-ink-jet printing; adhesion testing; tape peel test and button shear test; device to flexible substrate sintered ink assembly; fully-additive assembly

I. INTRODUCTION

Flexible microsystems are becoming more attractive due to their stretchability, bendability, foldability and twistability to be able to conform to a variety of complex surfaces. In the current phase of flexible electronics innovation, printed electronics is increasingly pursued in addition to patterned copper-flex technology. This printing brings new, low-cost, adaptable tooling for deposition of wide range of materials [1]. With a fully-additive process, overall cost decreases since the additive process does not require multistep lithography processing as in subtractive or semi-additive manufacturing.

Assembly of components on substrates with printed conductors is currently being pursued in academia as well as in industry. While traditional solder reflow is a key technology for assembly on rigid substrates with copper pads, the solder reflow does not work with most printed conductors. Also, solder reflow requires high-temperature processing which may not be amenable to several low-temperature polymer substrates typically used in flexible electronics. Printed electronics assembly with traditional tooling, mainly focuses on Ag paste and epoxy [2, 3]. For surface-mount device (SMD) attachments, many different options are available including anisotropic conductive films (ACF), isotropic conductive adhesives (ICA) or pastes and wire-bonding [4, 5]. ACFs are a well-established lamination-based technology and offer good electrical conductance. Also, the assembly process requires lower temperatures compared to typical solder reflow temperatures, and thus is amenable to low-temperature polymer substrates. However, the assembly process requires expensive Au bumps for good contact as well as high pressures for assembly. There are also limitations on the bump pitch, due to the particle spacing and size in the ACF to have good electrical contact without creating shorts. Conductive adhesive or paste may be dispensed or stencil-printed on die pads, and they would form spherical bumps which can be brittle. The bumps are created by dipping Au bumps into an adhesive and the bumps offer acceptable electrical conductance. In wire-bonding, Au wires are bonded to the die pad, swept, and then attached to the printed pads on the substrate. However, the printed pads need to be reinforced with electroless nickel immersion gold (ENIG) for the attachment of wirebonds.

Another process, called dielectric ramp, utilizes a printed dielectric ramp around the edges of a die to be able to print conductive traces from the die pads to the substrates, building both wiring and interconnections in a single step. In this process, the die is first attached to the substrate with its active side up before printing the dielectric ramp. [6, 7]. However, this technique limits the assembly mostly to peripheral pad layouts, requires a large footprint, and has higher electrical parasitics due to longer trace lengths.

For better pitch scalability and electrical performance, sintering technologies offers the best solution [8]. This work explores sintering of Ag ink as a way of assembling components on flexible substrates, since Ag ink can be directly sintered onto the trace without the metallic coating to protect the traces. Soldering directly onto the Ag trace would consume the Ag trace. Also, Ag ink is conductive

2377-5726/18/$31.00 ©2018 IEEE
DOI 10.1109/ECTC.2018.00064

after oxidizing as well as having sintering temperatures below 250 ºC [9].

The objectives of this work are three-fold: 1) To validate the quality of the printing process by measuring the adhesion strength of printed Ag ink conductor on a flexible substrate, for example, liquid crystal polymer (LCP), 2) To develop an innovative fully-additive sintering-based assembly process to attach a surface-mount device at low temperature on the flexible substrate, and 3) To determine the adhesion strength of the assembly through shear testing.

II. AG INK PRINTING AND ADHESION QUALIFICATION

Characterizing adhesion of printed thin films is challenging because it is often hard to debond the printed thin film from the substrate [10]. Many evaluations often use the qualitative ASTM D3359-17 test. Peel test has also been used to quantify the adhesion [9, 11, 12]. However, in some of these tests, an additional layer is added to the printed film to thicken it and be able to hold and peel the film. On the other hand, to assess assembly adhesion of components on substrates, shear adhesion of ink on substrates is a better indicator for final qualification over peel testing [10].

In this work, ink-jet printed Ag conductors on a flexible substrate were qualified by both ASTM D3359-17 test as well as button shear test. The results from such tests are presented here after an initial introduction to the ink attributes and curing.

A. Ag Ink Attriubutes

Typically, Ag inks are used for creating the conductive lines/traces, while pastes are used for joints formation [2, 13-16]. Understanding the sintering characteristics of the specific printed ink is key for a fully-additive assembly process where the same ink is used for the traces as well as for the device-to-substrate joints Few impacting factors to Ag ink similar to paste are: (a) processing parameters: deposition technique, sintering profile, and drying time (b) ink composition: Ag particle size, geometry and distribution/concentration and (c) design: layout and deposition path [17]. For this work, Suntronic™ EMD 5730 was used as it is ink-jet compatible with a low sintering range, 150-250 °C, and is appropriate for substrates that are stable in that temperature range. The ink consists of 40% weight concentration of 50 nm Ag particles in a solvent.

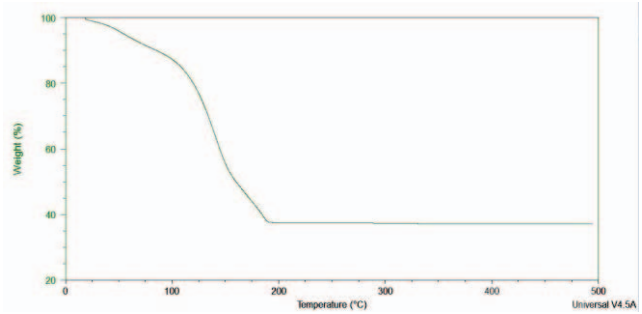

Figure 1: Residual weight of Suntronic Ink @ ramp rate of 10 °C/min with temperature run from room temperature to 500 °C

Using a TA Instrument SDT 600 analyzer (SDT-combination of Differential Scanning Calorimeter (DSC) and Thermogravimetric analyzer (TGA)), one can determine when the solvent fully evaporates by monitoring the weight loss in the printed ink. The experiment in Figure 1 was conducted at 10 °C/min ramping rate. Accordingly, it is seen in Figure 1 that the net weight of the ink after reaching a temperature of 200 °C is about 40% indicating that almost all of the solvent has evaporated by 200 °C, with only Ag left behind. Figure 2 shows the SEM image of Ag ink specimen after the solvent has evaporated, and as seen, the Ag conductor is porous. Although the initial characterization experiment was conducted to a temperature of 500 °C, subsequent studies for adhesion measurements were conducted with the silver ink sintered at 200 °C for 30 minutes, as would be practiced in an actual printing and sintering process.

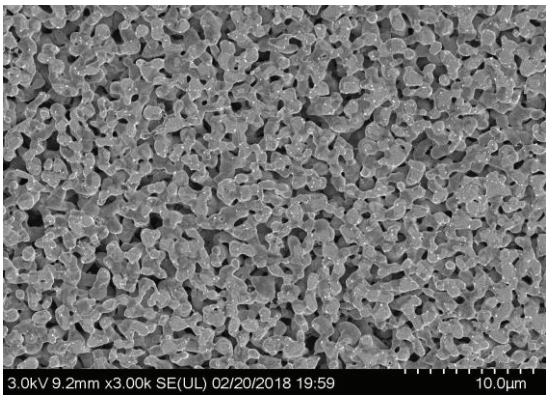

Figure 2: SEM image of Ag Ink after 20 C/min ramp from room to 500 °C

B. Ink Jet Printing on Flexible Substrate

Rogers Ultralam® 3850HT, a bare LCP substrate, was prepped by cleaning the surface with acetone followed by isopropyl alcohol (IPA) rinse. A commercial Fujifilm Dimatrix™ DMP 2831 ink jet printer was used to deposit SunChemical® SunTronic™ EMD 5730 on the LCP substrate. For the printer settings, the drop spacing was set at 25 µm, and the platform holding the LCP was set to 60 °C during the print. Multiple layers of 25.4 x 25.4 mm square designs were printed. The samples were then sintered in an oven for 30 min at 200 °C. Multiple layers of ink were printed, as each layer was about 2 µm in thickness after sintering, and thus, the total ink thickness was between 4 and 6 µm, depending on the number of ink layers. For ink-to-substrate adhesion qualification, two adhesion tests were used, as discussed below.

C. ASTM D3359-17 Tape Peel Test

ASTM D3359-17, a visual inspection adhesion test qualification test, was first performed on the Ag/LCP sample. In this test, a grid pattern was first scratched onto the printed ink to create a matrix of small ink squares, and a piece of tape was then adhered on top covering the entire grid pattern and held for 30-60 seconds. Then the piece of tape was peeled, and the number of small ink squares remaining on the substrate could be used as an indicator of

the adhesion strength. If 65% or more of the ink squares are removed from the substrate by the tape peel, then it is B0 (poor adhesion), and if none of the squares is removed, then it is B5 (excellent adhesion with no delamination) [18]. This test does not provide any force or interfacial fracture toughness information.

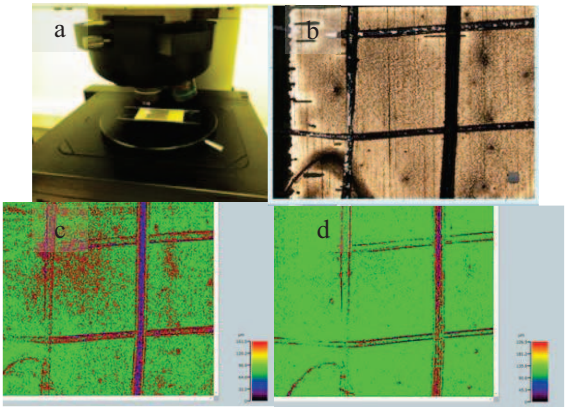

Figure 3: ASTM D3359-17 Visual inspection (a) Olympus LEXT 3D Laser Measuring Microscope (b) Optical view of sample and scratched grid (c) Profilometer view before tape peel test and (d) Profilometer view after tape peel test

Visual inspection was done with an Olympus® LEXT 3D laser measuring microscope as shown in Figure 3. The grid consisted of approximately 10 x 10 squares, and upon peeling using the tape test, practically all of the squares remained on the substrate indicating that the adhesion quality was of B5 standard. Figure 3b shows an example 2 x 2 square, as seen through the confocal microscope, out of the total of 10 x 10 squares. Figure 3c shows the laser profilometer view before the tape peel test, and Figure 3d shows the view after the test indicating that none of the ink squares peeled off.

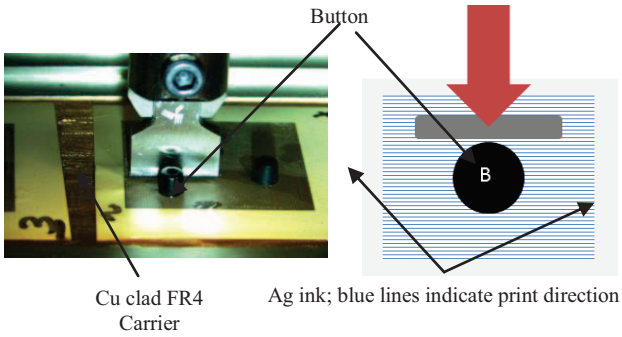

Figure 4: (a) Image of the button shear set-up (b) Schematic top view of shear button test with inkjet printed perpendicular to the printed path

D. Button Shear Test

The button shear test results are quantitative compared to the ASTM D3359-17 test. The shear button test set up is shown in Figure 4. For the button shear test, the flexible LCP was adhered to a carrier Cu-clad FR-4 board which was sized to fit into the vice of the shear tester. Next, preformed epoxy mold compound buttons were adhered to the ink's surface using a commercially available epoxy that is set at room temperature to cure. The room-temperature cure alleviates any concerns of microstructure change in the conductive ink, if the epoxy were to be cured at higher temperatures. Due to the print droplet spacing and the print head path, directionality was observed in the film along the direction the printer head's path and the samples were prepared to examine the interfacial shear strength perpendicular to the direction of the print. In the ongoing work, interfacial shear strength along the direction of print is also being examined.

Table 1: ID Test sample description

ID	Variables	
	# layers	*Thermal treatment*
1	3	N
2	2	N
3	3	Y
4	2	Y

Table 1 lists various test cases studied for the button shear test. As seen, two to three layers of ink with and without thermal treatment were examined through the button shear test. Figure 5 shows the SEM images of printed Ag that was thermally treated for 48 hours at 200 °C, and as seen, the Ag particles have fused well, seemingly on the top surface. Additional imaging studies are required to determine the layer effect of fusion. After 30-minute sintering, the structure is more similar to the one shown in Figure 2.

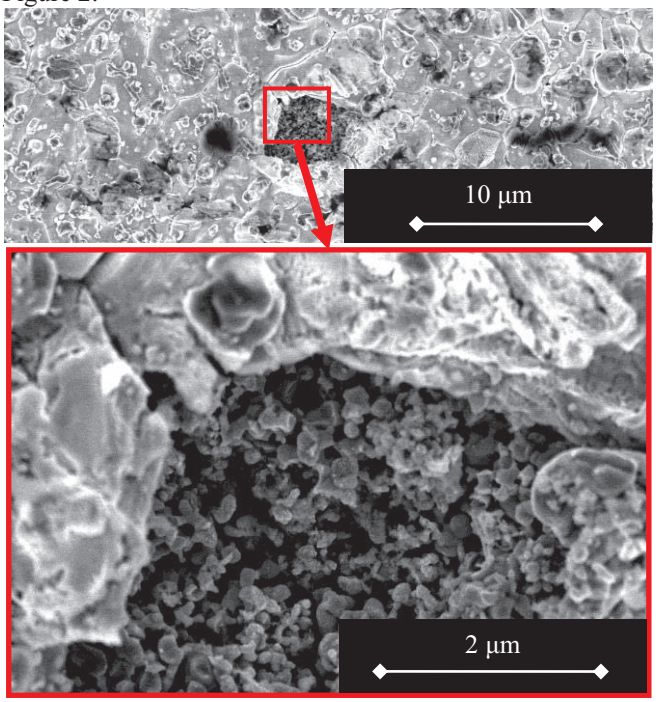

Figure 5: SEM image of a thermally-treated ink showing two distinct layers in Ag

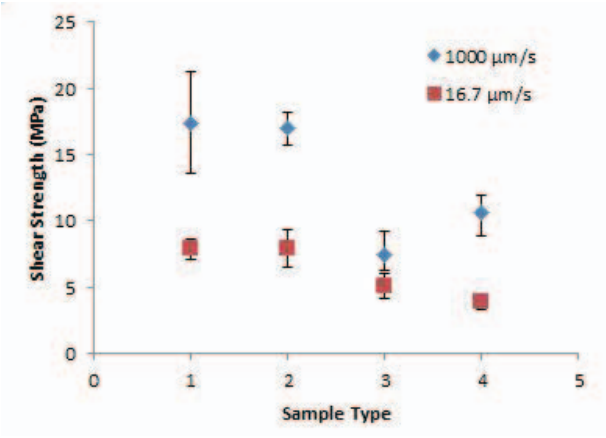

Figure 6: Button shear stress test results

Shear testing was done at 1000 µm/s as well as at 16.7 µm/s rates with a XYZtec™ Condor Sigma with zone shear attachment. Multiple samples were done for each test described in Table 1, and the results are shown in The button shear test results are quantitative compared to the ASTM D3359-17 test. The shear button test set up is shown in Figure 4. For the button shear test, the flexible LCP was adhered to a carrier Cu-clad FR-4 boar. The load at which the button is sheared off is divided by the area of the button to obtain the average shear strength. As seen, the number of layers did not influence the results. However, the thermal treatment seemed to have reduced the average shear strength by about 30% for 16.7 µm/s test and by about 50% for the 1000 µm/s test.

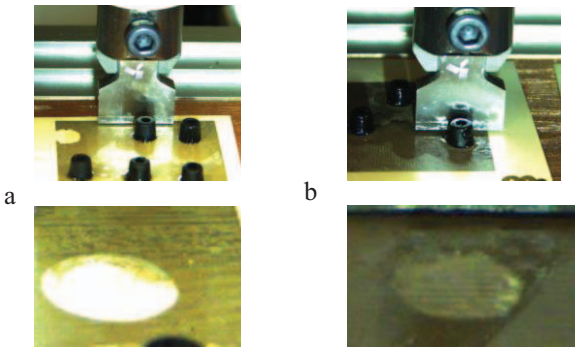

Figure 7: Shear testing (a) Delamination between Ag and LCP after initial print and oven sintered (b) Residual Ag on LCP indicating cohesive Ag failure after thermal treatment of ink

Upon examining the sheared surfaces, it is seen that thermally-untreated specimens have a clear delamination of the ink from the substrate, as shown in Figure 7a. However, the thermally-treated specimens have more of a cohesive fracture of the ink between layers of ink with different levels of fusion as shown in Figure 7b, and thus demonstrate a lower strength. The images in Figure 7 are for 1000 µm/s rate experiments. For shear tests conducted at 16.7 µm/s, the failure is often partially interfacial and partially cohesive due to the relatively slow speed of the test, and the shear strength values appear to be between the interfacial and cohesive fracture values. The SEM image in Figure 5, shows the two layers of Ag ink and this may explain the lower shear strength instead of increasing shear strength as expected in literature [19]. Several additional tests are being performed for further analysis and interpretation.

The adhesion results, discussed above, are specific to the ink and fabrication process. Printing has different factors to consider which can affect the adhesion, including the path and speed the tool head takes, placement of subsequent layers (direct versus off-set), and initial droplet size [12].

III. ASSEMBLY AND ADHESION EVALUATION

Ag ink trace assembly and die shear studies have been done elsewhere on various substrates, including paper, polyimide, and glass [3]. In their work, the authors have used solder, epoxy, or sintered ink for device assembly. In the sintered ink process, they deposit ink after the resistor is placed. Although depositing ink after device placement works for resistor with two pads, such a process is not likely to work for flip-chip applications which may have full area-array interconnects. A preferable procedure of assembly is to place the ink on the substrate pads, then place the component, and then sinter the entire assembly in an oven.

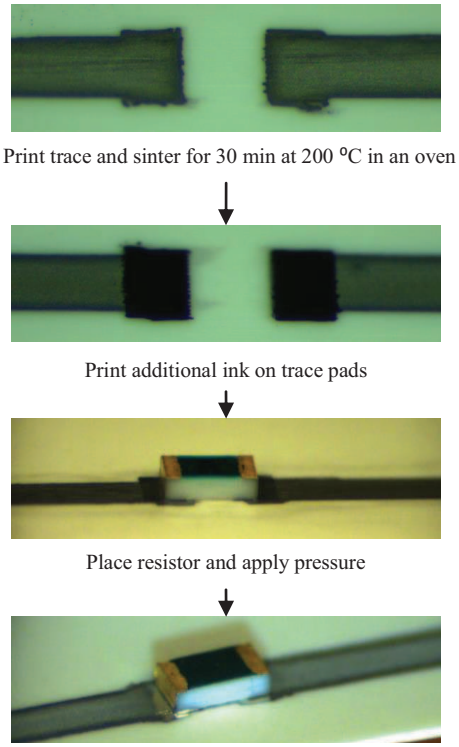

Figure 8: Full-ink assembly process

For assembly demonstration purposes, the samples assembled were 603 resistors with Au finished electrodes.

The process is for an initial evaluation of a fully-additive assembly process as an alternative to conventional solder flip-chip bonding. Although resistor assembly is demonstrated in this work, the long-term aim is to apply the assembly process for flip-chips and other packages in the future.

A. Assembly Process

Figure 8 shows the steps for the assembly process of the resistor. First, Ag traces with pad layouts were printed on an LCP flexible substrate and sintered at 200 ºC for 30 minutes. Additional Ag ink was then printed on the contact pads for assembly purposes. The resistor was then placed on the contact pads using a semi-automatic Finetech® Fineplacer® flip-chip bonder to ensure planarity and pressure control. Different compressive forces (0.2, 0.5, 1.0, 3.0, and 5.0 N) were applied on the resistors. The substrate with the resistors was then placed in a thermal oven to be sintered at 200 °C for different time durations (15, 30, 45, and 60 min), and no pressure was applied during the sintering.

B. Adhesion Strength of the Assembly

Die shear testing was done to compare the strength of the joints on XYZtec™ as shown in Figure 9. The die shear testing was done at a shearing rate of 16.7 µm/s. In Figure 9, the horizontal axis shows different sintering times, while the vertical axis shows the maximum shearing force as measured in XYZtec™. As seen, the higher forces during device placement generally lead to higher shearing forces indicating stronger device-to-substrate joints. However, for a given compressive force and for a given sintering time, there are variations in the maximum shear force. This is because multiple resistors were placed and assembled on a coupon of LCP flexible substrate, and there were warpage-induced non-coplanarity issues as to the location where the resistors were placed on the flexible substrate, and that location influenced shear force results. Also, it is seen from Figure 9 that the sintering time beyond 30 minutes did not influence the maximum shear force results.

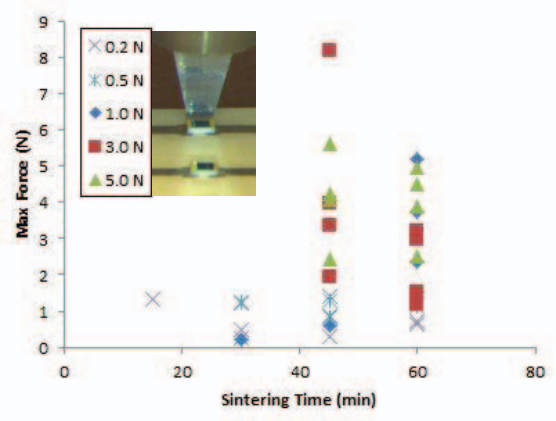

Figure 9: Shear results for different resistors placed with different forces (0.2, 0.5, 1.0, 3.0, and 5.0 N) and varying sintering times in an oven set at 200 °C. The image next to the legend shows a resistor about to be sheared.

Figure 10 shows four samples with pad and trace areas on the substrate side after shearing of resistors. The images are from test coupons that had been assembled with 5.0N force and 60 min sintering time at 200 ºC. In the images, bare LCP can be seen where the joints were sheared. This indicates that Ag ink got sheared off from the LCP substrate. This means that the Ag joint is stronger than the adhesion of the Ag to the LCP, and thus, the proposed assembly process appears to be a viable option.

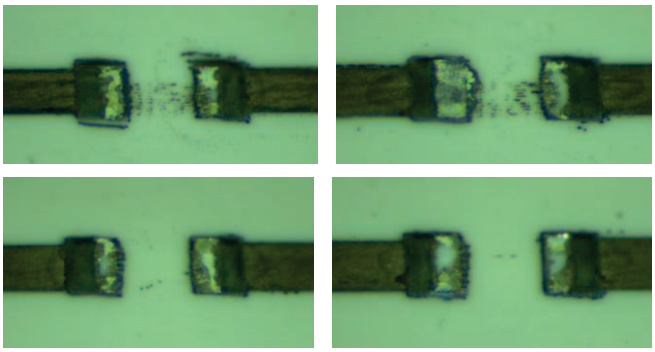

Figure 10: Shearing of assembled resistors (assembly parameters: 5.0 N force and 60 min sintering time) shows bare LCP substrate under the ink pad

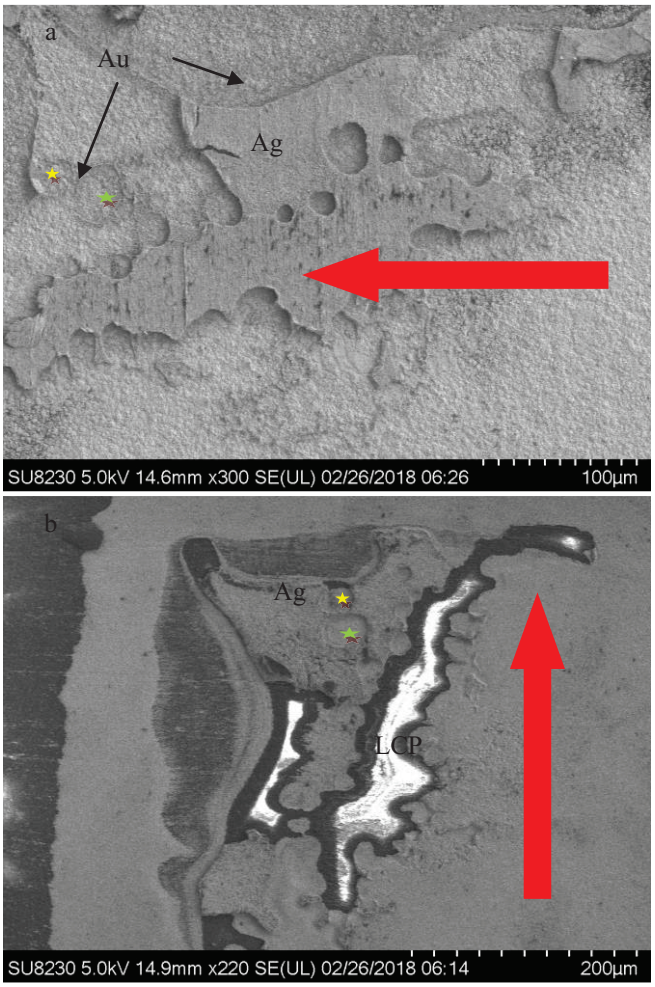

Figure 11: SEM images of resistor pad and substrate pad (a) Resistor pad showing Ag (b) Substrate pad showing LCP. Assembly placement force was 0.2 N. Sintering time was 45 min. EDX was done to ensure the identification of the interfaces; the red arrow corresponds to shear directions and the stars are to help orient how the resistor and substrate sides were sandwiched together.

Figure 11a shows the resistor pad and Figure 11b shows the substrate pad with EDX information. The images were taken after the shearing was completed. The images pertain to an assembly placement force of 0.2 N and an assembly sinter time of 45 min at 200 °C. As observed, Ag was still adhering to the resistor pad, while bare LCP was visible on the substrate pad indicating all of the Ag had been sheared away from that location during the die shear test. This result is somewhat similar to what is presented in Figure 10, where a larger portion of the bare LCP is seen on the substrate pad side. It should be emphasized that Figure 10 corresponds to a larger placement force of 5.0 N, while Figure 11 corresponds to a lower placement force of 0.2 N. The images in Figure 10 and Figure 11 confirm that with the larger placement force, the joint strength is greater than the adhesion strength of Ag ink to LCP. In the die shear tests, the shear head was kept sufficiently low to the substrate to minimize moment effects on the shearing area.

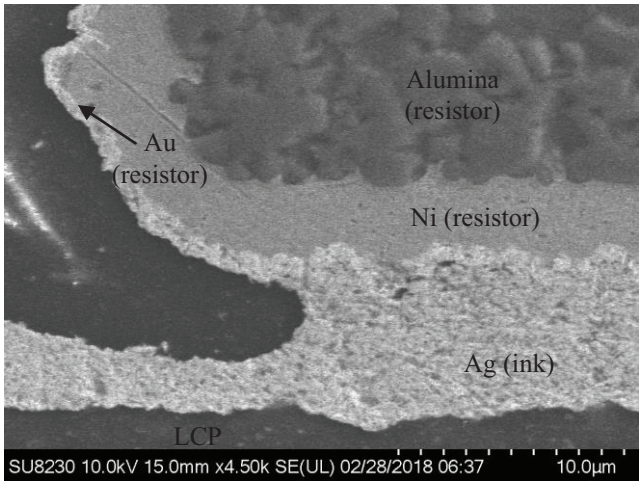

Figure 12: SEM of cross-section of the 1.0 N force for 60 minutes

Cross-sectioning was also done to see the quality of joint upon assembly, Figure 12 shows an alumina resistor with Ni/Au pad adhering to Ag in the joint and the trace printed on top of LCP. The total thickness of Ag is about 6 µm with 4 µm for the initial trace with two layers and 2 µm additional ink added for assembly purposes. As seen in the cross-section, the Ag ink did wet the resistor pad.

In another assembly, done with 0.5 N placement force, it is seen that the Ag from the initial trace and Ag from the subsequent joint did not fuse together during the assembly sintering process, as shown in Figure 13. It is possible that the ink might have dried prior to actual sintering due to logistics involved in terms of printing stations and assembly stations.

More work is being done to create Ag joints using a fully-additive process. However, based on these initial studies, it is promising that full-ink processing can produce Ag joints that are stronger than the adhesion strength of Ag to LCP.

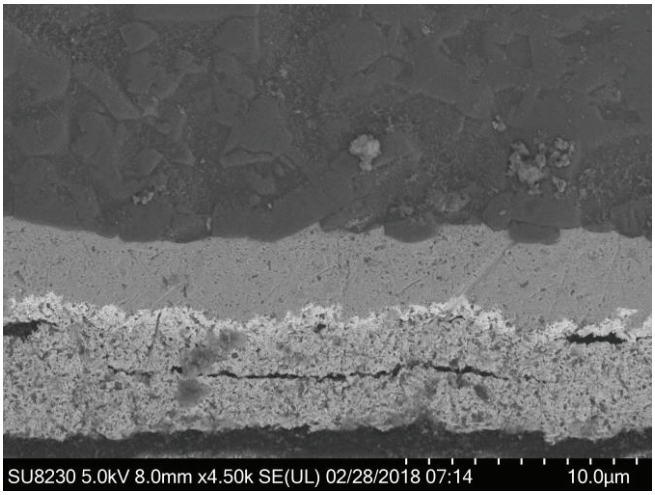

Figure 13: Cross-section of 0.5 N force at 60 min in oven at 200 °C shows that the ink did not always fuse with the Ag trace.

IV. CONCLUSION

In this work, Ag ink-jet printed films on a flexible substrate were qualified by both ASTM D3359-17 tape peel test and button shear test. When there was no additional thermal treatment after sintering the ink, the samples failed at the interface between the ink and LCP in the button shear test, and the shear strength was found to be 16 MPa. However, the ink exhibited cohesive failure when there was thermal treatment of the ink at 200 °C for 48 hours, and the shear strength dropped to 8 MPa.

Resistors were attached to Ag lines printed on LCP with a fully-ink process in a serial fashion: print and sinter traces, print ink pads, place resistor with a flip-chip bonder, and then place sample in an oven at 200 °C. This serial process appears to be a better approach, especially for area-array flip-chip assembly in the future. Also by having the wet ink only on the substrate side, there would be less assembly variations where the device pads are also wetted with the ink in a dip process prior to placement and sintering. Die shear testing results of the assembled resistors show that the shear strength of the joint is greater than the shear strength between the trace and LCP.

Various additional printing and assembly tests are ongoing. These include: studying the effect of print directionality on adhesion strength, peel testing of print traces and comparing the results with shear testing, and assembly of various other devices on different flexible substrate materials. It is anticipated that the demonstrated assembly technique is likely to be applicable to flip-chip and other package assemblies on flexible substrates. In addition to die shear testing, additional mechanical tests such as bending, twisting, stretching, etc. as well as environmental

tests such as thermal cycling, thermal storage, temperature/humidity, etc. need to be performed for successful qualification of the presented assembly technique.

ACKNOWLEDGMENT

This material is based, in part, on research sponsored by Air Force Research Laboratory under agreement number FA8650-15-2-5401, as conducted through the flexible hybrid electronics manufacturing innovation institute, NextFlex. The U.S. Government is authorized to reproduce and distribute reprints for Governmental purposes notwithstanding any copyright notation thereon. The views and conclusions contained herein are those of the authors and should not be interpreted as necessarily representing the official policies or endorsements, either expressed or implied, of Air Force Research Laboratory or the U.S. Government. The authors are appreciative to discussions with Boeing collaborators on the project. They would also like to thank the support provided by fellow members in the Packaging Research Center, Athena, and Computer-Aided Simulation of Packaging Reliability (CASPaR) Lab at Georgia Tech.

REFERENCES

[1] Z. Yin, Y. Huang, N. Bu, X. Wang, and Y. Xiong, "Inkjet printing for flexible electronics: Materials, processes and equipments," *Chinese Science Bulletin,* vol. 55, pp. 3383-3407, 2010.

[2] B. N. An, M. Kempf, B. Leyrer, T. Blank, J. Kolb, and M. Weber, "Evaluation of Ag-sinter pastes for the die attachment in power electronic modules using design of experiments," in *2016 18th European Conference on Power Electronics and Applications (EPE'16 ECCE Europe)*, 2016, pp. 1-10.

[3] J. Arrese, G. Vescio, E. Xuriguera, B. Medina-Rodriguez, A. Cornet, and A. Cirera, "Flexible hybrid circuit fully inkjet-printed: Surface mount devices assembled by silver nanoparticles-based inkjet ink," *Journal of Applied Physics,* vol. 121, p. 104904, 2017/03/14 2017.

[4] M. J. Yim, Y. Li, K.-s. Moon, K. W. Paik, and C. P. Wong, "Review of Recent Advances in Electrically Conductive Adhesive Materials and Technologies in Electronic Packaging," *Journal of Adhesion Science and Technology,* vol. 22, pp. 1593-1630, 2008/01/01 2008.

[5] R. Cauchois, M. Saadaoui, J. Legeleux, T. Malia, B. Dubois-Bonvalot, K. Inal*, et al.*, "Wire-bonding on inkjet-printed silver pads reinforced by electroless plating for chip on flexible board packages," in *3rd Electronics System Integration Technology Conference ESTC*, 2010, pp. 1-6.

[6] B. K. Tehrani, B. S. Cook, and M. M. Tentzeris, "Inkjet-printed 3D interconnects for millimeter-wave system-on-package solutions," in *2016 IEEE MTT-S International Microwave Symposium (IMS)*, 2016, pp. 1-4.

[7] J. Putaala, J. Niittynen, J. Hannu, S. Myllymäki, E. Kunnari, M. Mäntysalo*, et al.*, "Capability Assessment of Inkjet Printing for Reliable RFID Applications," *IEEE Transactions on Device and Materials Reliability,* vol. 17, pp. 281-290, 2017.

[8] J. Zürcher, K. Yu, G. Schlottig, M. Baum, M. M. V. Taklo, B. Wunderle*, et al.*, "Nanoparticle assembly and sintering towards all-copper flip chip interconnects," in *2015 IEEE 65th Electronic Components and Technology Conference (ECTC)*, 2015, pp. 1115-1121.

[9] K. Inyoung, L. Taik-Min, and K. Jongryoul, "A study on the electrical and mechanical properties of printed Ag thin films for flexible device application," *Journal of Alloys and Compounds,* vol. 596, pp. 158-63, 05/25 2014.

[10] S. C. Joo and D. F. Baldwin, "Analysis of Adhesion and Fracture Energy of Nano-Particle Silver in Electronics Packaging Applications," *IEEE Transactions on Advanced Packaging,* vol. 33, pp. 48-57, 2010.

[11] E. Halonen, T. Viiru, K. Ostman, A. L. Cabezas, and M. Mantysalo, "Oven Sintering Process Optimization for Inkjet-Printed Ag Nanoparticle Ink," *IEEE Transactions on Components, Packaging and Manufacturing Technology,* vol. 3, pp. 350-6, 02/ 2013.

[12] H. C. Jung, S.-H. Cho, J. W. Joung, and Y.-S. Oh, "Studies on Inkjet-Printed Conducting Lines for Electronic Devices," *Journal of Electronic Materials,* vol. 36, pp. 1211-1218, 2007/09/01 2007.

[13] K. S. Siow, "Are Sintered Silver Joints Ready for Use as Interconnect Material in Microelectronic Packaging?," *Journal of Electronic Materials,* vol. 43, pp. 947-961, 2014/04/01 2014.

[14] K. S. Siow, "Mechanical properties of nano-silver joints as die attach materials," *Journal of Alloys and Compounds,* vol. 514, pp. 6-19, 2/15/ 2012.

[15] J. Kahler, N. Heuck, A. Stranz, A. Waag, and E. Peiner, "Pick-and-Place Silver Sintering Die Attach of Small-Area Chips," *IEEE Transactions on Components, Packaging and Manufacturing Technology,* vol. 2, pp. 199-207, 2012.

[16] J. Yan, G. Zou, A.-p. Wu, J. Ren, J. Yan, A. Hu*, et al.*, "Pressureless bonding process using Ag nanoparticle paste for flexible electronics packaging," *Scripta Materialia,* vol. 66, pp. 582-585, 2012/04/01/ 2012.

[17] K. S. Siow and Y. T. Lin, "Identifying the Development State of Sintered Silver (Ag) as a Bonding Material in the Microelectronic Packaging Via a Patent Landscape Study," *Journal of Electronic Packaging,* vol. 138, pp. 020804-020804-13, 2016.

[18] A. D. Mulliken and M. C. Boyce, "Mechanics of the rate-dependent elastic–plastic deformation of glassy polymers from low to high strain rates," *International Journal of Solids and Structures,* vol. 43, pp. 1331-1356, 3// 2006.

[19] S. Egelkraut, L. Frey, M. Knoerr, and A. Schletz, "Evolution of shear strength and microstructure of die bonding technologies for high temperature applications during thermal aging," in *2010 12th Electronics Packaging Technology Conference*, 2010, pp. 660-667.